1963ApJ...138.1074S

EVOLUTION OF O STARS. I. HYDROGEN-BURNING

RICHARD STOTHERS
Harvard College Observatory and Goddard Institute for Space Studies,
National Aeronautics and Space Administration
Received May 25, 1963

ABSTRACT

The evolution of an O-type star of 30 $M_\odot$ is considered from its initial main-sequence state to the point where the hydrogen content of the core has decreased from 70 per cent to 7 per cent by weight. The O stars are characterized by convective instability in the envelope and the full CNO-cycle of energy generation. Radiation pressure is important throughout the star, and electron scattering dominates the opacity. The inhomogeneous models consist of four zones: (I) a radiative envelope retaining the initial composition, (II) an outer semiconvective zone with a continuously varying composition that has a discontinuity at the interface with (III) an inner radiative zone also with a continuously varying composition, and (IV) a homogeneous convective core. Due to increasing radiation pressure, the semiconvective zone grows more rapidly outward than inward, but produces little effect on the important stellar quantities. The mass fraction of the core decreases from 0.60 to 0.34 and the mean hydrogen content of the star gets 40 per cent depleted. The age, 4.7 million years, is shorter than that for other sequences computed for stars of mass $\approx 30\ M_\odot$ because of a higher luminosity. This is mainly the result of choosing a higher mean molecular weight and CNO content.

I. INTRODUCTION

It is believed that the early-type spectra of the H-R diagrams of very luminous OB clusters and associations can be explained by a main sequence of rapidly evolving massive stars. Schwarzschild and Härm (1959) showed that the upper end of the main sequence of stable stars may lie at about 60 $M_\odot$; this should correspond to the hottest of normal O5 spectra.

Sakashita, Ôno, and Hayashi (1959) have studied the evolution of a star with mass 15.6 $M_\odot$ and initial spectrum B0, and found a growing convective instability in the envelope. This instability does not occur in stars with mass $\lesssim 10\ M_\odot$ (Schwarzschild and Härm 1958) and remains negligible up to about the mass they chose. For more massive stars, however, it must be taken into account. Increasingly important is the role of O^{16} in the hydrogen-burning reactions. At temperatures above 3×10^7 ° K (the central temperature of the main-sequence model for a star of 15.6 $M_\odot$) the CNO-cycle replaces the CN-cycle. Thus we find characteristic of the O stars: (1) convective instability in the envelope and (2) the complete CNO-cycle.

The massive stars with $M \lesssim 10\ M_\odot$ have been discussed by several workers (Tayler 1954; Kushwaha 1957; Blackler 1958; Henyey, LeLevier, and Levée 1959; Hoyle 1960). These stars are characterized by a *shrinking* of their convective regions. Their evolution is perhaps best described by Kushwaha (1957).

In this paper we propose to study in detail the early evolution of a star with mass lying in the region of the O stars, heretofore studied only approximately (Blackler 1958; Schwarzschild and Härm 1958; Henyey *et al.* 1959; Hoyle 1960). We choose a mass of 30 $M_\odot$ and consider the evolution to the point where the hydrogen content of the core drops to 10 per cent of its initial value.

II. ASSUMPTIONS

The usual general assumptions are made.

1. Mass loss is neglected for the early evolutionary phases, following, for example, the summary by Deutsch (1960) and the note by Huang, Milligan, and Stecher (1962). Were mass loss significant, it should be easily observable (Mustel 1959), since even among the late-type giants where the surface gravity is much lower, mass loss is not always observed.

© American Astronomical Society • Provided by the NASA Astrophysics Data System

1963ApJ...138.1074S

2. Rotation is neglected. Although more massive stars on the main sequence are observed to rotate faster, supergiants have little or no rotation. Theoretical justification exists for the necessary braking during evolution (see, e.g., Huang and Struve 1960). Even rotation during the main-sequence phase probably produces little mixing, since the observed Trumpler effect in galactic clusters suggests evolution without mixing for many of the early-type stars (Deutsch 1960). In fact, theory predicts long time scales of mixing, and Mestel (1959) has calculated that there will be mixing between the core and envelope only if the star is near disruption. By neglecting rotation, we also neglect departures from spherical symmetry.

3. No convective overshooting and consequent mixing occurs between any of the convective-radiative interfaces in the star. Sakashita and Hayashi (1961) have discussed this assumption.

4. The turbulent mixing in the core is complete and maintains a steady homogeneity of composition.

Calculation of the structure of the star is considerably simplified by the following additional conditions.

1. The surface temperature of the O and early B stars is so high that the outer convection zone is negligible. This means that we may consider the envelope as in radiative equilibrium out to the boundary.

2. The convective core contains such a large fraction of the stellar mass that effectively all of the nuclear energy generation occurs there.

3. Degeneracy does not set in even at the center. If we may extrapolate the results of Hayashi and Cameron (1962) for a star of 15.6 $M_\odot$, the gas will remain non-degenerate at least up to the carbon-burning phase.

4. The opacity may be assumed with good accuracy to depend only on electron scattering (cf. Hayashi and Cameron 1962).

Appreciable structural complications occur in very massive stars, however. Radiation pressure must be fully taken into account throughout, and the inner part of the envelope becomes convectively unstable. Thus, simplification of the physics is offset by increasing structural difficulties.

III. GENERAL STRUCTURE

The internal structure of very massive stars is now fairly well understood, as the result of the accumulated efforts of several workers over the past few years. Following the work of Tayler (1954) and Kushwaha (1957) on stars of mass less than 10 $M_\odot$, in which a shrinking convective core leaves behind a radiative intermediate zone with continuous gradient of mean molecular weight, Schwarzschild and Härm (1958) showed that in stars of higher mass, radiation pressure makes the region just outside the core convectively unstable. Convection mixes the composition until the unstable zone attains convective neutrality. The resulting distribution of chemical composition was determined by equating the radiative and adiabatic temperature gradients.

Sakashita *et al.* (1959) pointed out that the existence of a gradient of mean molecular weight will in turn act to suppress the convective motion in the semiconvective zone. Therefore, a term including this gradient must be added to the adiabatic temperature gradient. They also showed that the predominance of electron scattering in the opacity requires the region at the boundary of the core to be in radiative equilibrium, in order to preserve continuity of the radiative energy flux. Assuming, however, that the convective motion in the intermediate zone is sufficiently effective, Sakashita and Hayashi (1959) discussed the case of a star of 46.8 $M_\odot$, in which the purely radiative zone does not appear because of overshooting mass motion. This may be true in the case where hydrogen has not been extensively depleted in the core, but eventually continuity of the radiative flux at the boundary of the core will require a radiative zone to form inside the semiconvective zone.

© American Astronomical Society • Provided by the NASA Astrophysics Data System

1963ApJ...138.1074S

Sakashita and Hayashi (1961) improved their model by dividing it into four zones: (I) a homogeneous radiative envelope retaining the initial composition, (II) a semi-convective outer intermediate zone, (III) a radiative inner intermediate zone, and (IV) a homogeneous convective core. In this paper their notation will be followed. We introduce the following subscripts: 0 for the boundary of the core in the initial model, 1 for the Interface I–II, 2 for the inner boundary of Zone II, 3 for the outer boundary of Zone III, and 4 for the Interface III–IV.

IV. PHYSICAL PARAMETERS

a) Chemical Composition

The initial composition at age zero is assumed to be

$$X_e = 0.70\ , \qquad Y_e = 0.27\ , \qquad Z_e = 0.03\ , \qquad X_{\mathrm{CNO}} = Z/2\ . \tag{1}$$

This is the same composition that Strömgren (private communication) uses for the upper main sequence. The CNO abundance was estimated from Cameron's (1959) revision of the Suess-Urey table of element abundances.

b) Opacity

The opacity is due to Thomson scattering by free electrons:

$$\kappa = 0.19(1 + X)\ . \tag{2}$$

c) Equation of State

The equation of state is

$$P = \frac{k}{\mu H}\,\rho T + \frac{a}{3}\,T^4\ . \tag{3}$$

d) Energy Generation

The most recent calculation of the energy-generation rate for the CNO-cycle is due to Reeves (1962), who used the results of Caughlan and Fowler (1962). The rate may be represented with sufficient accuracy for the temperatures of our models by

$$\epsilon = \epsilon_0 X X_{\mathrm{CNO}} \rho T^{\nu}\ , \tag{4}$$

with $\nu = 15$ and $\log \epsilon_0 = -106.6$. Actually, for the early models oxygen is not quite yet in equilibrium. This formula is accurate to within 15 per cent, the estimated probable error of the exact formula. The reaction $N^{14}(p, \gamma)O^{15}$ appears now to be non-resonant, so that the major uncertainty lies in the extrapolation of the experimental data on $O^{16}(p, \gamma)F^{17}$ to low energies. Fortunately, the badly known $O^{17}(p, \alpha)N^{14}$ rate does not significantly affect the energy generation for temperatures above 2×10^7 ° K (Reeves 1962).

It may be noted that the values of ϵ obtained from the formulae of Fowler (1960) and Burbidge, Burbidge, Fowler, and Hoyle (1957) are the same as Reeves's values to within 15 per cent, for the temperatures of our models.

V. BASIC EQUATIONS

The basic equilibrium equations are

$$-\frac{r}{P}\frac{dP}{dr} = \frac{GM(r)\rho}{rP} = V\ , \qquad \frac{r}{M(r)}\frac{dM(r)}{dr} = \frac{4\pi r^3 \rho}{M(r)} = U\ ,$$
$$\frac{T}{P}\frac{dP}{dT} = n + 1\ , \qquad \frac{dL(r)}{dM(r)} = \epsilon\ , \tag{5}$$

© American Astronomical Society • Provided by the NASA Astrophysics Data System

1963ApJ...138.1074S

where the radiative and adiabatic indices, n, are given by

$$(n+1)_{\text{rad}} = \frac{16\pi cG(1-\beta)M(r)}{\kappa L(r)}, \qquad (n+1)_{\text{ad}} = 4 - \frac{1.5\beta^2}{4-3\beta}. \tag{6}$$

In addition, we have the following two equations governing the distribution of chemical composition in Zones II and III, respectively:

$$\frac{1}{(n+1)_{\text{rad}}} = \frac{1}{(n+1)_{\text{ad}}} + \frac{\beta}{4-3\beta}\frac{d\log\mu}{d\log P}, \qquad \mu = \mu_\iota\left[\frac{M(r)}{M(r)_\iota}\right]^{-\lambda_\iota}, \tag{7}$$

where ι refers to the point at which the mass fraction is equal to that of the core of the previous model. The composition exponents λ_ι are discussed in the following section.

We introduce the following non-dimensional variables:

$$r = xR, \quad M(r) = qM, \quad P = pP_0, \quad T = tT_0 \quad \text{(Zones I–III)}, \tag{8}$$

$$r = x^*r_0, \quad M(r) = q^*M_0, \quad P = p^*P_c, \quad T = t^*T_c \quad \text{(Zone IV)}, \tag{9}$$

where

$$P_0 = \frac{GM^2}{4\pi R^4}, \quad T_0 = \frac{\mu_e HGM}{kR}, \quad r_0 = \frac{k}{\mu_c HT_c}\sqrt{\frac{3(1-\beta_c)}{4\pi Ga}}, \quad M_0 = r_0\frac{kT_c}{\mu_c HG}. \tag{10}$$

Then since effectively all the nuclear energy generation takes place in the core, we may set $L(r) = L$ in Zones I–III and obtain

$$\frac{dp}{dx} = -\frac{\beta pql}{x^2t}, \quad \frac{dq}{dx} = \frac{\beta px^2l}{t}, \quad \frac{dt}{dx} = -C\frac{\beta pj}{x^2t^4}, \quad \beta = 1 - A\frac{t^4}{p} \quad \text{(Zones I–III)}, \tag{11}$$

with

$$\frac{d\log l}{dx} = \left[\frac{d\log t}{dx} - \frac{1}{(n+1)_{\text{ad}}}\frac{d\log p}{dx}\right]\frac{4-3\beta}{\beta} \quad \text{(Zone II)}, \tag{12}$$

and

$$l = l_\iota\left(\frac{q}{q_\iota}\right)^{-\lambda_\iota} \quad \text{(Zone III)}, \tag{13}$$

where

$$l = \frac{\mu}{\mu_e}, \quad j = \frac{\mu}{\mu_e}\frac{1+X}{1+X_e}, \quad A = \frac{4\pi a}{3}\left(\frac{\mu_e H}{k}\right)^4 G^3M^2,$$
$$C = 0.19(1+X_e)\frac{3}{64\pi^2 ac}\left(\frac{k}{\mu_e HG}\right)^4\frac{L}{M^3}. \tag{14}$$

For the core we have

$$\frac{dp^*}{dx^*} = -\frac{\beta p^*q^*}{x^{*2}t^*}, \quad \frac{dq^*}{dx^*} = \frac{\beta p^*x^{*2}}{t^*}, \quad \frac{dt^*}{dx^*} = \frac{1}{(n+1)_{\text{ad}}}\frac{t^*}{p^*}\frac{dp^*}{dx^*},$$
$$\beta = 1 - (1-\beta_c)\frac{t^{*4}}{p^*} \quad \text{(Zone IV)}. \tag{15}$$

Given μ_e and M, the solutions of Zones I and II are specified by the luminosity parameter C. The solutions of Zone III require an additional parameter, the composition exponent λ. The core solutions are specified by β_c.

© American Astronomical Society • Provided by the NASA Astrophysics Data System

1963ApJ...138.1074S

To obtain the luminosity, we integrate the energy generation (eq. [4]) over the convective core:

$$L = \epsilon_0 X_c X_{\mathrm{CNO}} \left(\frac{\mu_e HG}{k}\right)^{\nu} \frac{M^{\nu+2}}{4\pi R^{\nu+3}} \left(\frac{x_4}{x_4^*}\right)^3 \left(\frac{p_4}{p_4^*}\right)^2 \left(\frac{t_4}{t_4^*}\right)^{\nu-2} \times l_c^2 \int_0^{x_4^*} \beta^2 p^{*2} t^{*\nu-2} x^{*2} dx^* . \tag{16}$$

Since L is determined directly from the parameter C, we can obtain R. Then all the physical variables in Zones I–III follow from the transformations, equations (8) and the first two equations of (10). The central temperature is obtained from $T_c = T_0 t_4/t_4^*$, whereupon all the physical variables in the core follow from equations (9) and the last two equations of (10).

Near the surface and center a starting series must be applied before beginning the integration of equations (11)–(15). We have

$$q = 1 , \qquad p = \frac{t^4}{4C}, \qquad t = \frac{\beta_0}{4}\left(\frac{1}{x} - 1\right), \qquad \beta_0 = 1 - 4AC \ \text{(surface)} \tag{17}$$

and

$$q^* = \tfrac{1}{3}\beta_c x^{*3}, \qquad p^* = 1 - \tfrac{1}{6}\beta_c^2 x^{*2}, \qquad t^* = 1 - \tfrac{1}{6}\frac{\beta_c^2}{(n+1)_c} x^{*2} \ \text{(center)} , \tag{18}$$

for x close to 1 and x^* small, respectively.

VI. CONSTRUCTION OF MODELS

The initial model contains only a radiative envelope and convective core, and is homogeneous throughout. Thereafter, an evolutionary sequence is produced by incrementing log C. The method of Sakashita and Hayashi (1961) has been followed. First, families of solutions are computed for Zone IV, characterized by β_c, and for Zone III, characterized by λ and fitted to Zone I as if there were no growing convective instability. Zone III is fitted to the core in U, V and $(n + 1)$. The semiconvective Zone II is now taken into account by reintegrating Zone I and adopting equations (12) when $(n + 1)_{\mathrm{rad}} = (n + 1)_{\mathrm{ad}}$. Since no nuclear reactions occur outside the core, the total amount of hydrogen and helium mixed must remain constant. Moreover, the convection will steepen the gradient of mean molecular weight near the Interface II–III, so that we make the approximation of specifying a discontinuity in μ here. The determination of q_2, which equals q_3, and fitting of the Zones II and III are made according to the conditions

$$\int_{q_1}^{q_2} (X_e - X_{\mathrm{II}})\, dq = \int_{q_0}^{q_3} (X_e - X_{\mathrm{III}})\, dq , \qquad \frac{U_3}{U_2} = \frac{V_3}{V_2} = \frac{\mu_3}{\mu_2} . \tag{19}$$

The inward growth of Zone III can be handled by a method described by Kushwaha (1957) for less massive stars. At the mass point q_i where the core of the previous model ended, Zone III is integrated inward with a new trial composition exponent λ_i, using the previous set of λ's for those outer subzones of Zone III not affected by mixing from the semiconvective zone. The integrations of Zone III are always begun with λ_0 at q_0, the mass fraction of the core in the initial model, and are fitted to a radiative envelope (Zone I) that is calculated without semiconvection.

The time step, $\Delta\tau$, is computed in the usual way (Schwarzschild 1958, p. 196).

VII. RESULTS AND DISCUSSION

Table 1 contains the results for the initial homogeneous model and four inhomogeneous models in which the zones were integrated with the help of an IBM 7090 computer but fitted by hand. The fitting on the $U - V$ plane is shown in Figure 1, where the dots

© American Astronomical Society • Provided by the NASA Astrophysics Data System

1963ApJ...138.1074S

log p_i	0.705	0.747			0.910	0.842			1.316	0.959			1.977	0.979			2.122
log t_i	−0.530	−0.506			−0.458	−0.461			−0.323	−0.410			−0.123	−0.402			−0.082
β_i	0.844	0.823			0.809	0 783			0.740	0.735			0.645	0.727			0.627
X_i	0.700	0.700	0 699	0 693	0.583	0.700	0.691	0.667	0.373	0.700	0 664	0.611	0 112	0.700	0.657	0.600	0.069
log C	−3.563	−3.500				−3 400				−3.300				−3.285			
λ	...	1.02				1.127				1.264				1.35			
β_c	0.768	0 738				0 678				0.594				0.578			
log T_c	7.562	7.573				7.594				7 635				7.649			
log ρ_c	0.482	0 486				0.508				0.610				0.650			
log $(L/L_\odot)$	5.148	5.211				5.311				5 411				5 426			
log $(R/R_\odot)$	0.817	0.855				0.943				1.090				1.118			
log T_e	4.639	4.635				4.616				4.568				4.558			
$\overline{X}$	0 700	0.633				0.527				0.420				0 405			
τ (10^6 years)	0.00	1.33				3 09				4.50				4.67			

TABLE 1

EVOLUTIONARY MODELS OF A STAR OF 30 $M_\odot$ DURING HYDROGEN-BURNING

	Model 0	Model 1				Model 2				Model 3				Model 4			
i	0	1	2	3	4	1	2	3	4	1	2	3	4	1	2	3	4
U_i	1.59	1.36	1.41	1.42	1.66	1.04	1.13	1.15	1.72	0.763	0.824	0.861	1.73	0.725	0.775	0.812	1.71
V_i	4.25	4.28	4.02	4.04	3.96	4.26	3.62	3 69	3 62	4.22	3 18	3.32	3.50	4.22	3 12	3.27	3.51
$(n+1)_i$	3.27	3.34			3.38	3.44			3.54	3.55			3 70	3.56			3.72
log x_i	−0.394	−0.413			−0.453	−0.453			−0.579	−0.502			−0.794	−0.510			−0.842
log q_i	−0.222	−0.203	−0.224	−0.224	−0.262	−0.178	−0.233	−0.233	−0.338	−0 152	−0.252	−0.252	−0.446	−0.148	−0.256	−0.256	−0.466

© American Astronomical Society • Provided by the NASA Astrophysics Data System

1963ApJ...138.1074S

and discontinuities represent fitting points. The zones outside the core are marked off by dashed lines (not to be confused with the lines representing the assumed radiative zone that becomes semiconvective). Only the core solution for $\beta = 1$ is plotted, for the sake of clarity.

The change of mass contained in each zone during the course of the star's evolution is shown in Figure 2. It is interesting to note that while the semiconvective zone grows rapidly outward, it moves inward only slightly. Figure 2 and Table 1 show also that by the time the hydrogen content of the core has dropped to 10 per cent of its initial value, both the mass fraction of the core and the mean hydrogen content of the whole star, $\bar{X}$, have decreased by about 40 per cent.

In Figures 3 and 4 the hydrogen content is plotted as a function of mass fraction for the evolutionary models here considered. Dots and the vertical discontinuities represent fitting points. Clearly, the decrease of X through the semiconvective zone is far more

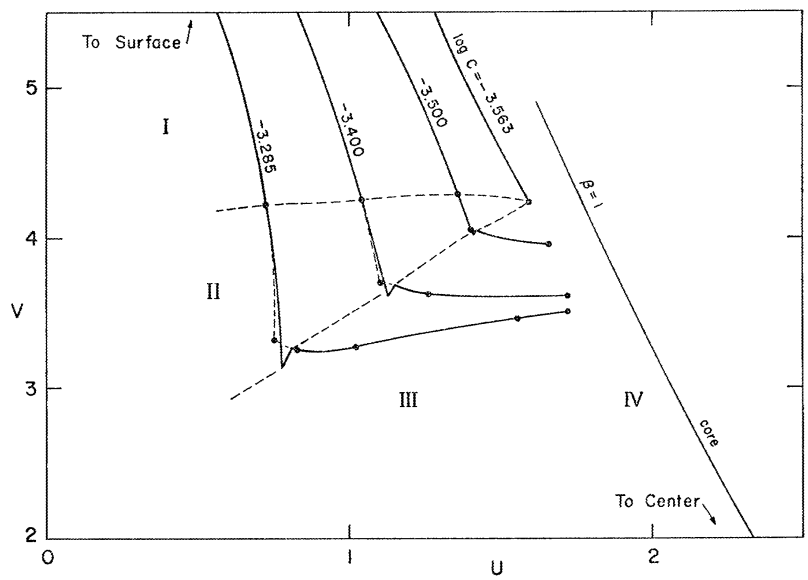

FIG. 1.—Evolution of the model sequence in the $U - V$ plane. The envelope solutions are designated by their log C values. Dots and jumps represent the fitting points. The extended dashed lines separate the zones, which are designated by Roman numerals. The dashed lines in the solutions represent the assumed radiative zone.

gentle than its decrease in the radiative intermediate zone; this is to be expected from the mixing process. The jump in mean molecular weight at the interface grows to about 5 per cent in the last model. Eventually, the discontinuity may no longer be considered a good approximation. However, it is clear that the semiconvective zone has little effect on the important quantities L, T_e, q_4, X_c, β_c, and T_c.

Figure 5 shows a luminosity-temperature plot of the evolutionary tracks of our model (30 $M_\odot$) and the model calculated by Sakashita *et al.* (15.6 $M_\odot$) to roughly the same amount of hydrogen depletion in the core. The more massive star has an initially steeper rise in luminosity, due to the greater mass fraction contained in the energy-producing core. When the discrepancy between the measured ultraviolet fluxes of early-type stars (Stecher and Milligan 1962) and those predicted on the basis of model atmospheres is resolved, it will be possible to compare our results with the observations of OB clusters and associations.

Several other workers have considered the evolution of stars with mass $\approx 30\ M_\odot$. In Table 2 we have summarized the data on the initial model ($X_c = X_e$) and a later

© American Astronomical Society • Provided by the NASA Astrophysics Data System

1963ApJ...138.1074S

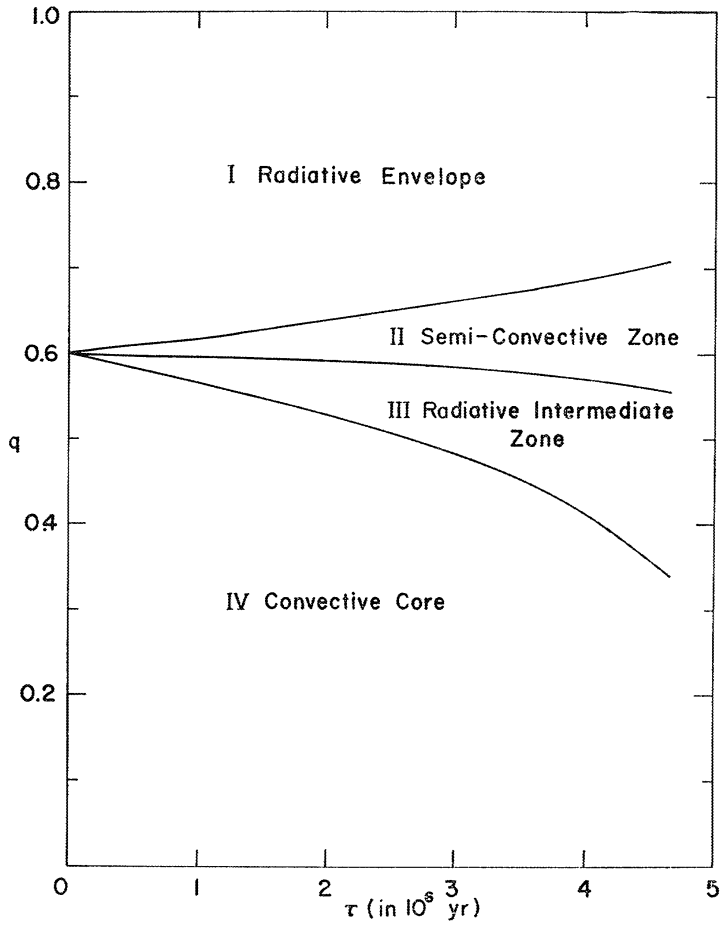

FIG. 2.—Evolution of the structural zones in a star of 30 $M_\odot$ during hydrogen-burning

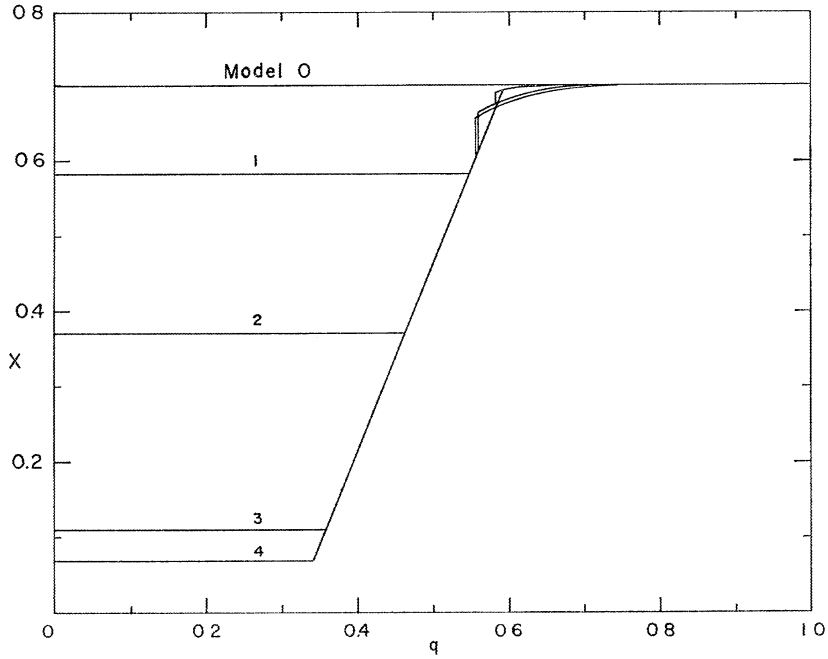

FIG. 3.—Depletion of hydrogen as a function of mass fraction for the evolutionary models of a star of 30 $M_\odot$.

© American Astronomical Society • Provided by the NASA Astrophysics Data System

1963ApJ...138.1074S

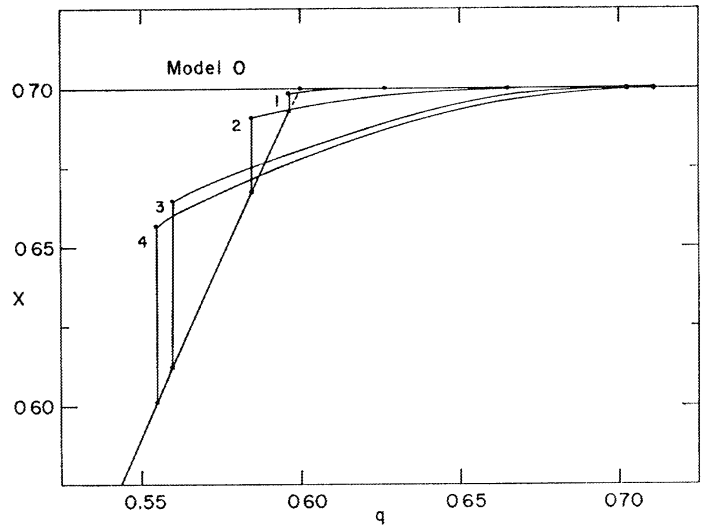

FIG. 4.—Detail of the depletion of hydrogen in the semiconvective zone for evolutionary models of a star of 30 $M_\odot$.

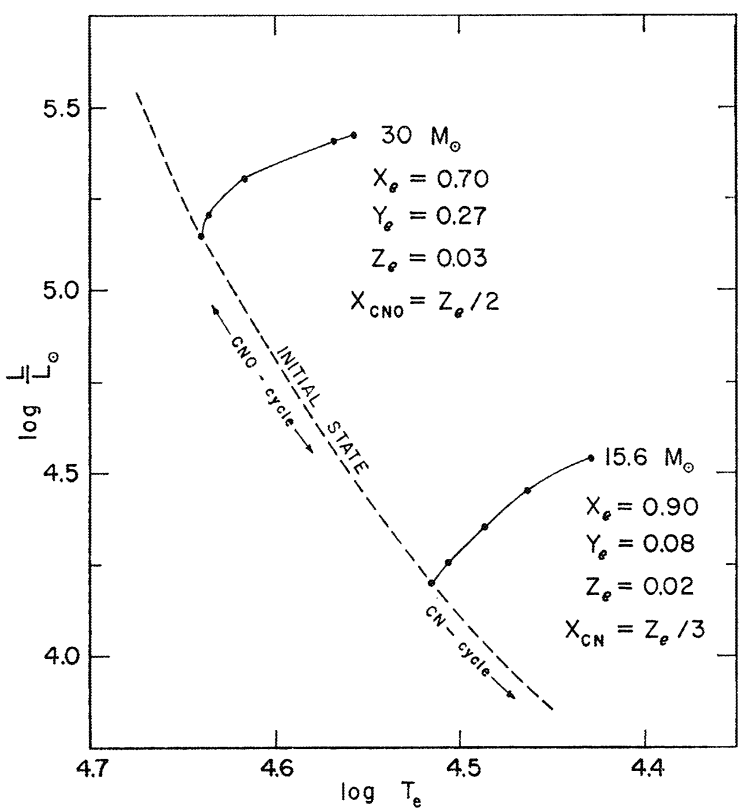

FIG. 5.—The evolution of stars of 30 $M_\odot$ (this paper) and 15.6 $M_\odot$ (Sakashita, Ôno, and Hayashi 1959) is compared on a plot of luminosity versus effective temperature.

© American Astronomical Society • Provided by the NASA Astrophysics Data System

1963ApJ...138.1074S

model ($X_c = \frac{1}{3}X_e$), whenever the later model was given or calculable by interpolation in the given sequence. The various models are arranged in order of chemical composition (toward older Population I), based primarily on the initial hydrogen content and secondarily on the metals content. We have by the last equation of (14), $L \approx \mu_e^4 M^3$ for an opacity due solely to electron scattering, and have listed the quantity $\mu_e^4 M^3$, normalized to the first entry in Table 2. Comparison with the trend of log $(L/L_\odot)$ is reasonably good. The small differences are due to differences in the chosen surface boundary conditions, opacity, nuclear energy generation, and method of integrating the basic equations. Moreover, because of increasing radiation pressure the mass-dependence of L is more like $M^{2.5}$ at 30 $M_\odot$ (Haselgrove and Hoyle 1959).

The arrangement of models in order of decreasing luminosity is fortuitously the same as that in order of decreasing CNO abundance, except for the rather anomalous model of

TABLE 2

COMPARISON OF EVOLUTIONARY MODEL SEQUENCES FOR STARS WITH $M \approx 30\ M_\odot$

Source	$X_c = X_e$								$X_c = \frac{1}{3}X_e$		
	M ($M_\odot$)	X_e	Y_e	Z_e	X_{CNO}	$\mu_e^4 M^3$	log $L/L_\odot$	log T_e	log $L/L_\odot$	log T_e	τ (10^6 yr)
Henyey, LeLevier, and Levée (1959)	30	0.68	0.31	0.01	0.0025	1.00	5.121	4.604	5.32	4.56	3.4
Stothers (1963)	30	.70	.27	.03	.0150	0.95	5.148	4.639	5.37	4.59	4.0
Schwarzschild and Härm (1958)	28.2	.75	.22	.03	.0043	0.68	5.035	4.630	5.30	4.57	5.2
Hoyle (1960)	30.1	.75	.23	.02	.0053	0.82	5.093	4.644	5.38	4.59	5.4
Haselgrove and Hoyle (1959)	30.2	.75	.24	.01	.0053	0.82	5.080	4.635	.		.
Blackler (1958)	32	.76	.2375	.0025	.0025	0.94	5.018	4.621	. .	. . .	. .
Blackler (1958)	32	0.85	0.1475	0.0025	0.0025	0.73	4.938	4.598	5.2	4.56	6.3

Henyey *et al.* (1959). But since the CNO abundance regulates the rate of energy generation and varies by a factor of six in Table 2, it can considerably alter the rate of consumption of hydrogen fuel. The change of time scale can better be seen by the following consideration of the total luminosity. Since $\mu_e \sim X^{-1}$ for small Z, $L \sim X^{-4}$ for approximately equal masses. Then $\tau \sim XL^{-1}$ or $\tau \sim X^5$, which gives the evident trend in the last column of Table 2.

Work is currently in progress on the further evolution of a star of 30 $M_\odot$ into the gravitational contraction phase during hydrogen exhaustion.

It is a pleasure to thank Dr. Hong-Yee Chiu and Dr. Leo Goldberg for advising this work. Dr. Martin Schwarzschild kindly offered some initial suggestions, and Dr. Robert Jastrow generously made available the facilities of the Institute for Space Studies. I gratefully acknowledge holding a Harvard scholarship during the academic year 1962–63.

REFERENCES

Blackler, J. M. 1958, *M.N.*, **118**, 37.
Burbidge, E. M., Burbidge, G. R., Fowler, W. A., and Hoyle, F. 1957, *Rev. Mod. Phys.*, **29**, 547.
Cameron, A. G. W. 1959, *Ap. J.*, **129**, 676.
Caughlan, G. R., and Fowler, W. A. 1962, *Ap. J.*, **136**, 453.
Deutsch, A. J. 1960, *Stellar Atmospheres*, ed. J. L. Greenstein (Chicago: University of Chicago Press), p. 543.
Fowler, W. A. 1960, *Modèles d'étoiles et évolution stellaire* (extrait des *Mém. Soc. R. Sci. Liège*, 5th ser., Vol. 3), p. 207.
Haselgrove, C. B., and Hoyle, F. 1959, *M.N.*, **119**, 112.
Hayashi, C., and Cameron, R. C. 1962, *Ap. J.*, **136**, 166.
Henyey, L. G., LeLevier, R., and Levée, R. D. 1959, *Ap. J.*, **129**, 2.
Hoyle, F. 1960, *M.N.*, **120**, 22.
Huang, S.-S., Milligan, J. E., and Stecher, T. P. 1962, *Pub. A.S.P.*, **74**, 312.

© American Astronomical Society • Provided by the NASA Astrophysics Data System

1963ApJ...138.1074S

Huang, S.-S., and Struve, O. 1960, *Stellar Atmospheres*, ed. J. L. Greenstein (Chicago: University of Chicago Press), p. 321.
Kushwaha, R. S. 1957, *Ap. J.*, **125**, 242.
Mestel, L. 1959, *Ninth International Symposium, Liège*, p. 235.
Mustel, E. R. 1959, *I.A.U. Symposium* (Paris), **10**, 20.
Reeves, H. 1962, *Stellar Energy Sources* (Institute for Space Studies, NASA report).
Sakashita, S., and Hayashi, C. 1959, *Prog. Theoret. Phys.* (Kyoto), **22**, 830.
———. 1961, *ibid.*, **26**, 942.
Sakashita, S., Ôno, Y., and Hayashi, C. 1959, *Prog. Theoret. Phys.* (Kyoto), **21**, 315.
Schwarzschild, M. 1958, *Structure and Evolution of the Stars* (Princeton, N.J.: Princeton University Press).
Schwarzschild, M., and Härm, R. 1958, *Ap. J.*, **128**, 348.
———. 1959, *ibid.*, **129**, 637.
Stecher, T. P., and Milligan, J. E. 1962, *Ap. J.*, **136**, 1.
Tayler, R. J. 1954, *Ap. J.*, **120**, 332.

© American Astronomical Society • Provided by the NASA Astrophysics Data System